Semiconductor Optoelectronics
ISSN: 1001-5868

THE DISTINCTIVENESS OF TURBULENCE ABOVE THE INDIAN MST RADAR IN THE TROPOSPHERE AND LOWER STRATOSPHERE

Rajendra Prasad Rao[*1], Amrees Pandey[1], Aditya Kumar Singh[1], Prakhar Yadav[1], R.S.Yadav[1]

[1] Department of Electronics & Communication, University of Allahabad, Prayagraj, India
rajendra.rao434@gmail.com, amrishpandey19@gmail.com, aditya08129@gmail.com, prakharwini@gmail.com, rsyadav_au@rediffmail.com
***Corresponding Email:** rajendra.rao434@gmail.com

Abstract: At Gadanki (13.5°N, 79.2°E), a tropical site on the Indian MST radar, turbulence characteristics were seen in the troposphere and lower stratosphere. The study depends on turbulence detection by using Thorpe analysis to the temperature profile while taking into account the effects of ambient moisture and sensor noise on static stability. Most of the time and space the tropospheric turbulence is intermittent. The lower troposphere from 3 to 8 km is substantially less turbulent than the altitude zone immediately adjacent to the convective tropopause (15–20 km). Over the COT, the rate of turbulence considerably reduces; occasionally, a relatively thin layer of turbulence is present (thickness o1 km). Although the persistent characteristics that may be seen in the 5–15 km altitude range are wide turbulent layers with a thickness of 42 km. Gadanki's turbulence strength between 5 and 15 kilometres above sea level is typically greater than Trivandrum's below 15 kilometres. The convective instability at Gadanki is the key factor controlling the turbulence. Strong wind clippers are the main cause of the turbulence, even if dynamic instability in the lower stratosphere dominates turbulence creation above 15 km.

Keywords: Turbulence, Indian MST radar

1. Introduction

According to measurements of pressure, temperature, and wind, the Upper Troposphere and Lower Stratosphere region experiences both large- and small-scale turbulence [1-4]. Numerous elements that affect the environment in that area, including radiation, atmospheric dynamics, and cloud microphysics, are to blame for the perturbations [5-6]. Convection and turbulence are two atmospheric phenomena that are crucial to the vertical mixing of air there. They control the interchange of air between the troposphere and stratosphere, as well as the vertical distribution of trace species and particles [7-13]. Dynamic instabilities are thought to be the primary cause of small-scale atmospheric turbulence. Gravity waves' dispersion and breaking can also cause turbulence. Highly erratic in both space and time, atmospheric turbulence [14-15]. In the atmospheric diffusion process, it may have a significant impact. Modeling the vertical distribution of trace elements in the UTLS region relies heavily on the turbulence parameters and turbulent kinetic energy dissipation rate [16-17]. Over the past few decades,

numerous experimental methods for calculating atmospheric turbulence parameters have been developed [18]. They include the utilisation of information from on-site probes attached to aeroplanes, rockets, and balloons, as well as turbulence remote sensing employing Indian MST radars [19-20]. The application of the Thorpe approach, which applies the ideas found in studies of ocean mixing to atmospheric data [21]. Based on the aforementioned theories on turbulence scaling, they suggested using the global high resolution radiosonde data set to infer the space-time variability of turbulence in the free atmosphere [22-23]. The values of were comparable with the right order of magnitudes and similar changeability with altitude when the turbulent kinetic energy dissipation rate from radiosonde data was compared with those determined using MST radar [24]. Both the measured values' orders of magnitude and the fluctuations in altitude were in good agreement. MST radars allowed for the long-term measurement of turbulence parameters in the troposphere, lower stratosphere, and mesosphere [25-26]. The majority of the reports on the climatological characteristics of turbulent diffusivity in the UTLS region deduced from MST radar readings were from mid-latitudes [27-30]. With the exception of a few studies employing the Indian MST radar, such investigations are fairly rare above the tropics [31]. The seasonal variability of turbulence parameters in the troposphere, lower stratosphere, and mesosphere over the Indian Monsoon region has been studied using data collected over three years from the MST Radar at Gadanki (13.5°N, 79.2°E) [32]. The ADP method was used to estimate the turbulent kinetic energy dissipation rate in the troposphere and stratosphere. Based on three years of radiosonde ascents at Gadanki, the seasonal fluctuation of turbulence parameters could only be observed until 17:30 IST [33-34]. During the summer monsoon period of 1999, an effort was made to define the feature of turbulence characteristics using the sparse dataset of MST radar observations from this station [35]. In this study, we use simultaneous high resolution radiosonde ascents conducted at two stations in the Indian MST radar Gadanki (13.5°N, 79.2°E) for more than three years between December 2010 and March 2014 to characterise the characteristics of turbulence in the troposphere and lower stratosphere [36-37]. In order to distinguish the distinctive characteristics of turbulence at these two locations during various seasons, the current study primarily focuses on the variability of turbulence in the UTLS region [38].

2. Observations and data

From December 2010 to March 2014, GPS were launched from Gadanki (13.5°N, 79.2°E) at intervals of three hours for three days in each month to research the sub-daily variability of winds in the troposphere and stratosphere. During the summer monsoon season, the tropical easterly jet stream from the Bay of Bengal region is a sign of the upper troposphere of Gadanki. With a basic vertical resolution of 4-6 m, GPS offers precise sampling of the zonal and meridional wind components over an altitude range of 0-35 km. Wind speed measurement precision is 0.15 m s—1. By launching the three different types of radiosondes simultaneously, their data's interdependence has been examined. The data from these sondes are discovered to agree quite well within the accuracy bounds. Before further processing, the data samples taken at 1-second intervals are submitted to a quality check. The following faults are removed from the profiles in this analysis: I Profiles that end at altitudes lower than 19 km; (ii) those that have missing data consistently for more than a kilometre. For the evaluation of turbulent characteristics, the radiosonde sounding profiles produced under convective instability

conditions are completely eliminated.

3. Parameter estimation of turbulence from temperature data

Based on turbulence scaling concepts for oceanic mixing that were built on the theory that the potential temperature grows monotonically with height in a stable environment, high resolution radiosonde measurements are used to estimate turbulence parameters. With this technique, the measured potential temperature profile is reconfigured into a steady monotone profile devoid of overturns. The Thorpe displacement is defined as the difference in height between a data bin in the observed and sorted profiles. The Thorpe displacement is the result of moving a sample from an initial altitude of Zn to an altitude of Zm during sorting. It should be emphasised that this approach can only be used in the environment when the atmosphere is statically stable. As a result, only stratified turbulence can be inferred using the underlying hypothesis to infer or K using this method. Numerous papers describing the use of the Thorpe method to detect turbulence in the troposphere and stratosphere using in situ atmospheric data have been published. The fact that none of these investigations account for the saturation of water vapour in the detection of turbulence is a significant problem, recent research has demonstrated that a hazy or water-vapour-rich atmosphere can have a major impact on the detection of turbulence. From a numerical integration of the dry Brunt-Väisälä frequency for sub-saturated air and the moist Brunt-Väisälä frequency for saturated air, they created a "composite potential temperature" (denoted by n).

4. Stability parameter estimation using MST radar data

The gradient Richardson number (Ri), which is a widely used parameter to indicate the presence of turbulence, is given by Ri14 N2/|U/h|2, where N is the BV frequency calculated from the actual potential temperature profile, |U/h| is the vertical gradient of horizontal vector wind U, and h is the altitude. N2 will be negative and N will be unknowable for the static instability. When Ri is less than 0.25, turbulence is thought to be a possibility. The following factors are typically thought to be necessary for the onset and maintenance of turbulence: I Rio1 is generally regarded as the condition needed to maintain wind-shear driven turbulence; (ii) Rio0.25 is thought to be the critical factor for turbulence onset; and (iii) Rio0 is favourable for the formation of convective instabilities. The horizontal wind gradient is calculated as |U/h|14[(du/ dh)2(dv/dh)2]1/2 from the zonal (u) and meridional (v) components of the horizontal wind U, where du/dh and dv/dh are the vertical gradients of zonal and meridional velocities, respectively. Calculating the horizontal wind gradient or wind shear at a height of 20 metres yields the shear in ms—1/m, which is then multiplied by 1000 to provide the shear in ms—1 km—1. In order to determine the Brunt-Väisälä (BV) frequency and Richardson number, it is necessary to take into account how moisture affects static stability and how noise from the measuring equipment affects temperature readings.

Code for figure 1

```
% edit MatrixHeader and Matrix for different data and save plots

MatrixHeader=['Height   '; 'Signal   ']
```

```
Matrix=[
3.60  4.247e-001
6.00  6.723e-001
8.40  2.428e-003
10.80  3.007e-004
13.20  3.239e-005
15.60  6.844e-005
18.00  6.656e-005
20.40  7.979e-006
22.80  7.629e-006
25.20  4.492e-00
27.60  7.017e-006
30.00  9.140e-006
32.40  1.227e-005
34.80  6.630e-006
37.20  8.827e-006
39.60  7.960e-006
42.00  1.201e-005
44.40  5.487e-006
46.80  9.844e-006
49.20  1.013e-005
51.60  7.246e-006
54.00  6.639e-006
56.40  7.670e-006
58.80  4.023e-006
61.20  4.710e-006
63.60  1.203e-005
66.00  4.238e-006
68.40  7.090e-006
70.80  6.544e-005
73.20  5.991e-006
75.60  1.030e-005
78.00  4.113e-006
80.40  1.008e-005
82.80  5.474e-006
85.20  1.090e-005
87.60  6.003e-006
90.00  8.009e-006
92.40  6.355e-006
94.80  5.534e-006
97.20  6.985e-006
]

M=Matrix'
```

```
[r,c]=size(MatrixHeader)
for i= 1:r
   var=MatrixHeader(i,:)
   if i==1
      figure
      grid on
      xlabel(var)

      leg=[]
   end
   if i>1
      hold on
      plot(M(1,:),M(i,:))
      leg=[leg;var]
   end
end
legend(leg)
```

Code for figure 2

```
% edit MatrixHeader and Matrix for different data and save plots

MatrixHeader=['Height   ';    'SNR(dB)  ']
Matrix=[
3.60    29.01
6.00    28.67
8.40   8.00
10.80    0.74
13.20    -9.53
15.60   -5.48
18.00   -4.91
20.40    -15.54
22.80    -14.98
25.20   -16.42
27.60    -14.82
30.00    -12.98
32.40   -12.87
34.80    -14.69
37.20    -13.86
39.60    -13.42
42.00    -12.76
44.40    -15.75
46.80    -13.35
49.20    -13.31
```

```
51.60    -15.74
54.00   -15.54
56.40    -14.21
58.80    -17.27
61.20    -16.35
63.60    -12.52
66.00    -17.26
68.40  -15.40
70.80   -6.12
73.20    -16.72
75.60   -13.31
78.00   -17.17
80.40   -13.22
82.80   -14.98
85.20   -13.43
87.60   -15.29
90.00   -13.14
92.40    -15.58
94.80   -15.35
97.20    -14.79
]

M=Matrix'
[r,c]=size(MatrixHeader)
for i= 1:r
   var=MatrixHeader(i,:)
   if i==1
      figure
      grid on
      xlabel(var)

      leg=[]
   end
   if i>1
      hold on
      plot(M(1,:),M(i,:))
      leg=[leg;var]
   end
end
legend(leg)
```

Code for figure 3

```
  % edit MatrixHeader and Matrix for different data and save plots
```

MatrixHeader=['Height '; 'Signal '; 'Doppler '; 'Width '; 'Noise Lev'; 'SNR(dB) ']
Matrix=[
3.60 4.247e-001 7.49e-002 3.80e-001 4.166e-006 29.01
6.00 6.723e-001 -3.13e-001 5.20e-001 7.137e-006 28.67
8.40 2.428e-003 -5.00e-001 5.92e-001 3.006e-006 8.00
10.80 3.007e-004 -6.45e-001 2.83e-001 1.979e-006 0.74
13.20 3.239e-005 1.89e-001 5.14e-001 2.270e-006 -9.53
15.60 6.844e-005 6.18e-001 1.57e-001 1.888e-006 -5.48
18.00 6.656e-005 4.96e-001 3.02e-001 1.612e-006 -4.91
20.40 7.979e-006 2.01e+000 2.28e-001 2.234e-006 -15.54
22.80 7.629e-006 5.64e+000 2.41e-001 1.876e-006 -14.98
25.20 4.492e-006 -5.49e+000 2.49e-003 1.540e-006 -16.42
27.60 7.017e-006 -5.98e+000 4.22e-003 1.661e-006 -14.82
30.00 9.140e-006 -2.05e+000 1.41e-001 1.419e-006 -12.98
32.40 1.227e-005 -4.53e+000 2.91e-001 1.854e-006 -12.87
34.80 6.630e-006 -7.32e-001 4.93e-004 1.525e-006 -14.69
37.20 8.827e-006 -3.96e+000 2.12e-001 1.679e-006 -13.86
39.60 7.960e-006 -3.21e+000 1.86e-001 1.366e-006 -13.42
42.00 1.201e-005 -2.45e+000 8.56e-002 1.771e-006 -12.76
44.40 5.487e-006 -6.10e-001 2.98e-004 1.610e-006 -15.75
46.80 9.844e-006 -2.50e+000 1.58e-001 1.662e-006 -13.35
49.20 1.013e-005 -5.29e+000 2.18e-001 1.696e-006 -13.31
51.60 7.246e-006 3.59e+000 1.81e-001 2.123e-006 -15.74
54.00 6.639e-006 3.65e+000 2.55e-001 1.856e-006 -15.54
56.40 7.670e-006 -1.71e+000 2.91e-004 1.581e-006 -14.21
58.80 4.023e-006 -3.17e+000 3.67e-004 1.675e-006 -17.27
61.20 4.710e-006 -6.30e+000 2.33e-001 1.588e-006 -16.35
63.60 1.203e-005 5.98e+000 1.08e-003 1.678e-006 -12.52
66.00 4.238e-006 -3.66e-001 0.00e+000 1.763e-006 -17.26
68.40 7.090e-006 -1.71e+000 8.74e-002 1.921e-006 -15.40
70.80 6.544e-005 3.08e-002 3.67e-001 2.093e-006 -6.12
73.20 5.991e-006 -3.05e+000 4.56e-004 2.199e-006 -16.72
75.60 1.030e-005 2.97e+000 2.68e-001 1.725e-006 -13.31
78.00 4.113e-006 -3.54e+000 1.04e-003 1.674e-006 -17.17
80.40 1.008e-005 4.95e+000 4.28e-001 1.653e-006 -13.22
82.80 5.474e-006 -1.34e+000 5.27e-004 1.347e-006 -14.98
85.20 1.090e-005 9.21e-001 2.36e-001 1.876e-006 -13.43
87.60 6.003e-006 4.52e+000 2.25e-003 1.584e-006 -15.29
90.00 8.009e-006 -3.99e+000 2.01e-001 1.289e-006 -13.14
92.40 6.355e-006 5.25e+000 1.60e-003 1.794e-006 -15.58
94.80 5.534e-006 5.00e+000 1.42e-003 1.481e-006 -15.35
97.20 6.985e-006 4.64e+000 4.10e-003 1.643e-006 -14.79
]

```
M=Matrix'
[r,c]=size(MatrixHeader)
for i= 1:r
   var=MatrixHeader(i,:)
   if i==1
      figure
      grid on
      xlabel(var)

      leg=[]
   end
   if i>1
      hold on
      plot(M(1,:),M(i,:))
      leg=[leg;var]
   end
end
legend(leg)
```

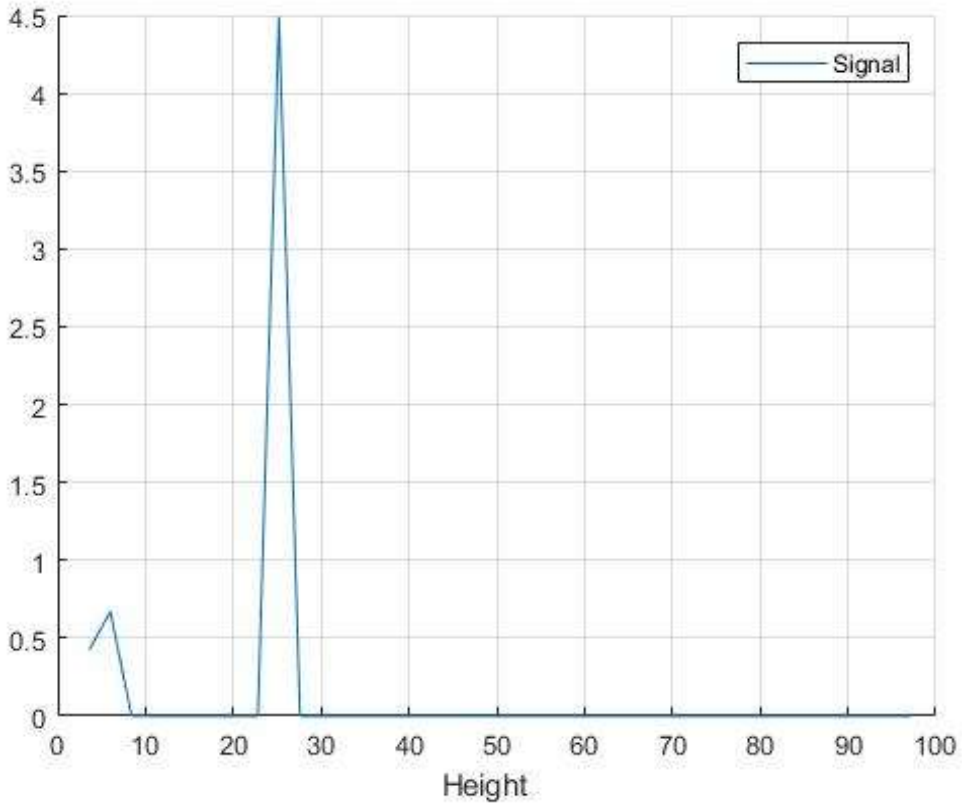

Figure 1: Shows the height versus signal graph

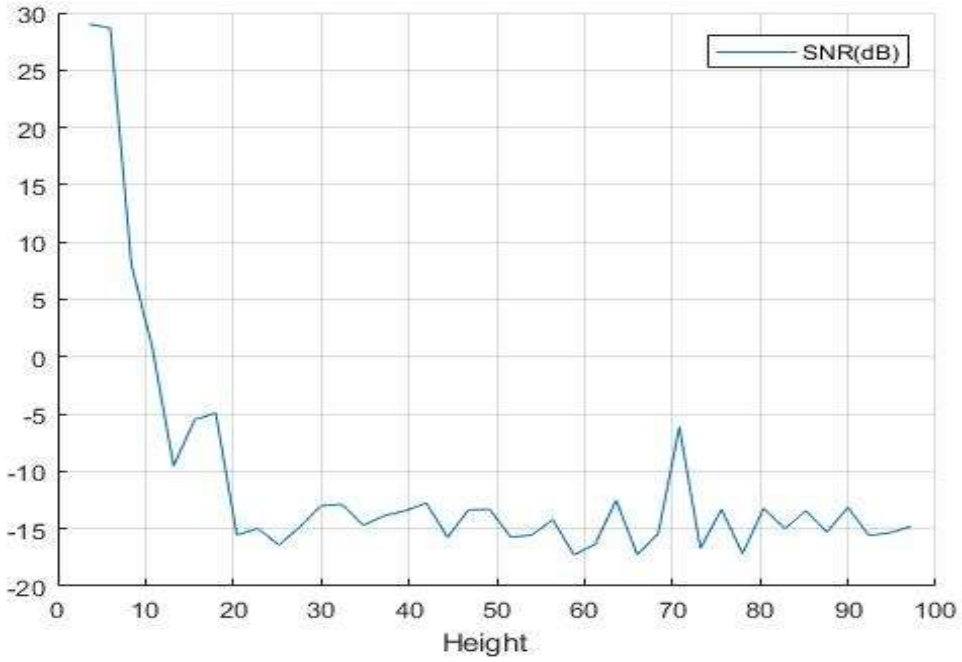

Figure 2: Shows the height versus SNR graph

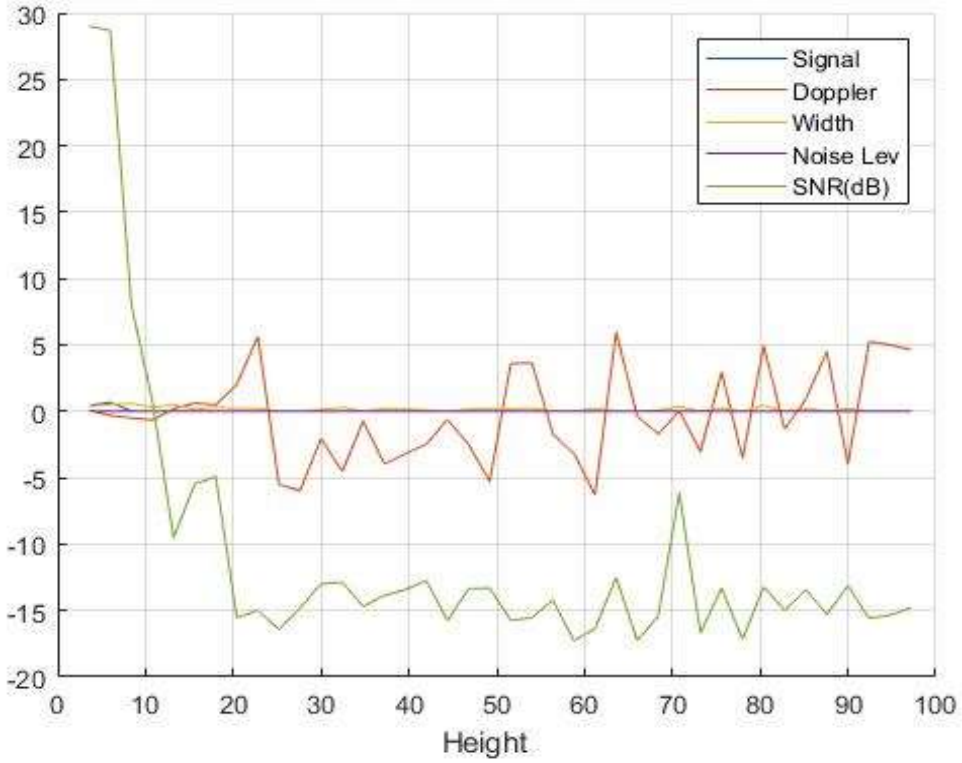

Figure 3: Shows the height versus signal, Doppler, width, noise level, and SNR graph

5. Conclusion

Using high resolution radiosonde data acquired at the one tropical station, Gadanki between December 2010 and March 2014, turbulence characteristics in the troposphere and lower stratosphere are studied. An application of a Thorpe analysis to potential temperature profiles is necessary for the discovery of turbulence. Stability parameters like N2 and Ri and turbulent parameters like LT,, and K are calculated while taking into account the effects of moisture and sensor noise on static stability and turbulence detection. The one station's altitude structure and contrasting tropospheric turbulence characteristics are identified. Despite the fact that the troposphere is turbulent in general, it is discovered that the turbulence is highly intermittent and discontinuous in both space and time. High levels of turbulence occur in the height range of 10-15 km, and their frequency is comparable to that of the ABL. However, the zone between (3-8 km) is comparatively less turbulent. The TTL region experiences extremely little turbulence, with the lowest levels being in the stratosphere. The frequency of N2 occurrences is exhibited by a broad peak in the altitude region of 10-15 km, with comparatively few occurrences in the altitude region of 3–8 km. While the likelihood of N2 sharply declines over 15 km, the likelihood of large wind shear increases. At Gadanki, the likelihood of wind shear exceeding 15 ms-1 km-1 is relatively low below 15 km. The Thorpe scale (LT) of turbulent overturns in the troposphere ranges from 20 to 1200 m, with the majority of them falling between 20 and 800 m. In about 45% of the cases at Gadanki, Thorpe scales are 200 m. The small-scale characteristics of several turbulent layers are revealed by the turbulence's altitude structure, especially in the lower troposphere. The surface characteristics and topographic factors are the key determinants of this turbulence. Mesoscale meteorology is crucial in determining the dynamics of the boundary layer and turbulence.

6. Acknowledgment

This research is done as a part of the Indian Space Research Organization's CAWSES-India program's Tropical Tropopause Dynamics (TTD) experiment (ISRO). For their tireless efforts in carrying out the tests, the authors are grateful to the technical and scientific employees of the SPL (Space Physics Laboratory), METF (Meteorology Facility), VSSC (Vikram Sarabhai Space Centre), and NARL (National Atmospheric Research Laboratory). In order to conduct this research, Dr. K. Parameswaran would like to thank the Indian CSIR (Council of Scientific and Industrial Research) for its assistance through the Emeritus Scientist programme. M. The ISRO research fellowship assists Muhsin. The authors acknowledge the anonymous reviewers for their insightful comments that helped to improve the manuscript.

References

[1] Alappattu, D.P., Kunhikrishnan, P.K., 2010. First observations of turbulence para- meters in the troposphere over the Bay of Bengal and the Arabian Sea using radiosonde. J. Geophys. Res. 115, D06105. http://dx.doi.org/10.1029/ 2009JD012916.

[2] Alexander, S.P., Tsuda, T., 2007. Measurements of vertical eddy diffusivity across the tropopause using radio acoustic sounding system (RASS). Geophys. Res. Lett. 34, L06803. http://dx.doi.org/10.1029/2006GL028753.

[3] Balsley, B.B., Kantha, L., Colgan, W., 2010. On the use of Slow Ascent Meter-Scale Sampling (SAMS) radiosondes for observing overturning events in the free atmosphere.J. Atmos. Ocean. Technol. 27, 766–775. http://dx.doi.org/10.1175/2009JTECHA1310.1.

[4] Cho, J., Newell, Y.N., Anderson, R.E., Barrick, B.E., Thornhill, J.D., Lee, K., Characterizations of tropospheric turbulence and stability layers from aircraft observations. J. Geophys. Res. 108 (D20), 8784. http://dx.doi.org/10.1029/ 2002JD002820.

[5] Clayson, C.A., Kantha, L., 2008. On turbulence and mixing in the free atmosphere inferred from high-resolution soundings. J. Atmos. Ocean. Technol. 25, 833–849. http://dx.doi.org/10.1175/2007JTECHA992.1.

[6] Duck, T.J., Whiteway, J.A., 2005. The spectrum of waves and the turbulence at the tropopause. Geophys. Res. Lett. 32, L07801. http://dx.doi.org/10.1029/ 2004GL021189.

[7] Fueglistaler, S., Dessler, A.E., Dunkerton, T.J., Folikins, I., Fu, Q., Mote, P.W., 2009. Tropical tropopause layer. Rev. Geophys. 47, RG1004. http://dx.doi.org/10.1029/ 2008RG000267.

[8] Ghosh, A.K., Jain, A.R., Sivakumar, V., 2003. Simultaneous MST radar and radiosonde measurements at Gadanki (13.5°N, 79.2°E) 2. Determination of various atmo- spheric turbulence parameters. Radio Sci. 38, 1014. http://dx.doi.org/10.1029/ 2000RS002528.

[9] Grubisic, V., et al., 2008. The terrain-induced rotor experiment. Bull. Am. Meteorol. Soc. 89, 1513–1533. http://dx.doi.org/10.1175/2008BAMS2487.1.

[10] Hocking, W.K., 1988. Two years of continuous measurements of turbulence para- meters in the upper mesosphere and lower thermosphere made with 2 MHz radar, J. Geophys. Res. 91, 2475–2491.

[11] Hocking, W.K., Mu, K.L., 1997. Upper and middle tropospheric kinetic energy dis-sipation rates from measurements of Cn_2-review of theories, in-situ in- vestigations, and experimental studies using the buckland park atmospheric radar in Australia. J. Atmos. Terr. Phys. 59, 1779–1803.

[12] Holton, J.R., Haynes, P.H., McIntyre, M.E., Douglass, A.R., Rood, R.B., Pfister, L., Stratosphere–troposphere exchange. Rev. Geophys. 33, 403–439.

[13] Kantha, L., Hocking, W., 2011. Dissipation rates of turbulence kinetic energy in the free atmosphere: MST radar and radiosondes. J. Atmos. Sol.-Terr. Phys. 73, 1043–1051.

[14] Keller, J.L., 1990. Clear air turbulence as a response to mesoscale and synoptic-scale dynamic processes. Mon.Weather Rev. 118, 2228–2242.

[15] Kirkwood, S., Mihalikova, M., Rao, T.N., Satheesan, K., 2010. Turbulence associated with mountain waves over Northern Scandinavia – a case study using the ES- RAD VHF radar and the WRF mesoscale model. Atmos. Chem. Phys. 10, 3583–3599.

[16] Kurosaki, S., Yamanaka, M.D., Hashiguchi, H., Sato, T., Fukao, S., 1996. Vertical eddy diffusivity in the lower and middle atmosphere: Climatology based on the MU radar observations during 1986–1992. J. Atmos. Sol. Terr. Phys. 58, 727–734.

[17] Lane, T.P., Reeder, M.J., Clark, T.L., 2001. Numerical modeling of gravity wave gen- eration by deep tropical convection. J. Atmos. Sci. 58, 1249–1274.

[18] Lübken, F.J., Rapp, M., Hoffmann, P., 2002. Neutral air turbulence and temperatures in the vicinity of polar mesosphere summer echoes. J. Geophys. Res. 107, 9-1–9- 10. http://dx.doi.org/10.1029/2001JD000915.

[19] Luce, H., Mega, T., Yamamoto, M.K., Yamamoto, M., Hashiguchi, H., Fukao, S., Nishi, N., Tajiri, T., Nakazato, M., 2010. Observations of Kelvin-Helmholtz instability at a cloud base with the middle and upper atmosphere (MU) and weather radars. J. Geophys. Res.115,D19116. http://dx.doi.org/10.1029/2009JD013519.

[20] Luce, H., Fukao, S., Dalaudier, F., Crochet, M., 2002. Strong mixing events observed near the tropopause with the MU radar and highresolution balloon techniques. J. Atmos. Sci. 59, 2885–2896.

[21] Mehta, S.K., Krishna Murthy, B.V., Rao, D.N., Ratnam, M.V., Parameswaran, K., Ra- jeev, K., Suresh Raju, C., Rao, K.G., Identification of tropical convective tropopause and its association with cold point tropopause. J. Geophys. Res, 113, D00B04. http://dx.doi.org/10.1029/2007JD009625.

[22] Miles, J.W., Howard, L.N., 1964. Note on heterogeneous flow. J. Fluid Mech. 20, 331–336.

[23] Murphy, E.A., D'agostino, R.B., Noonan, J.P., 1982. Patterns in the occurrence of Ri-chardson numbers less than unity in the lower atmosphere. J. Appl. Meteorol. 21, 321–333.

[24] Nastrom, G.D., Eaton, F.D., 2005. Seasonal variability of turbulence parameters at 2 to 21km from MST radar measurements at Vandenberg Air Force Base, Cali- fornia. J. Geophys. Res, 110, D19110. http://dx.doi.org/10.1029/2005JD005782.

[25] Nastrom, G.D., Eaton, F.D., 1997. Turbulence eddy dissipation rates from radar ob- servations at 5–20km at White Sands Missile Range, New Mexico. J. Geophys. Res. 102, 19495–19505.

[26] Nath, D., Venkat Ratnam, M., Patra, A.K., Krishna Murthy, B.V., Bhaskar Rao, S.V., 2010. Turbulence characteristics over tropical station Gadanki (13.5°N, 79.2°E) estimated using high-resolution GPS radiosonde data. J. Geophys. Res. 115, D07102. http://dx.doi.org/10.1029/2009JD012347.

[27] Parameswaran, K., krishna Murthy, B.V., Rose, K.O., Satyanarayana, M., 1993. Lidar studies of troposheric aerosol extinction and estimation of vertical eddy dif- fusion coefficient at a tropical station. Ann. Geophys. 11, 61–67.

[28] Pavelin, E.G., Whiteway, J., 2002. Gravity wave interactions around the jet stream. Geophys. Res. Lett. 29 (21), 2024. http://dx.doi.org/10.1029/2002GL015783.

[29] Rao, D.N., Venkat Ratnam, M., Rao, T.N., Rao, S.V.B., 2001b. Seasonal variation of vertical eddy diffusivity in the troposphere, lower stratosphere and meso- sphere over a tropical station. Ann. Geophys. 19, 975–984.

[30] Rao, D.N., Rao, T.N., Venkataratnam, M., Tulasiraman, S., Rao, S.V.B., 2001a. Diurnal and seasonal variability of turbulence parameters observed with Indian MST radar. Radio Sci. 36, 1439–1457.

[31] Rao, T.N., Radhakrishna, B., Satyanarayana, T.M., Kumar, S.S., 2010. The exchange across the tropical tropopause in overshooting convective cores. Ann. Geophys. 28, 113–122.

[32] Ratnam, M.V., Sunilkumar, S.V., Parameswaran, K., Krishna Murthy, B.V., Ramku- mar, G., Rajeev, K., Basha, G., Babu, S.R., Muhsin, M., Mishra, M.K., Kumar, A.H., Raj, S.T.A., Pramitha, M., Tropical tropopause dynamics (TTD) campaigns over Indian region: an overview. J. Atmos. Terr. Phys. 121, 229–239.

[33] Roper, R.G., 1996. Rocket vapor trail releases revisited: turbulence and the scale of gravity waves: implications for the imaging Doppler interferometry/incoherent scatter radar controversy. J. Geophys. Res, 101 (D3), 7013–7018.

[34] Satheesan, K., Krishna Murthy, B.V., 2002. Turbulence parameters in the tropical troposphere and lower stratosphere. J. Geophys. Res, 107 (D1), 4002. http://dx. doi.org/10.1029/2000JD000146.

[35] Schneider, A., Gerding, M., Lübken, F.-J., 2015. Comparing turbulent parameters obtained from LITOS and radiosonde measurements. Atmos. Chem. Phys. 15, 2159–2166.

[36] Smyth, W.D., Moum, J.N., 2000. Length scales of turbulence in stably stratified turbulence. Phys. Fluids 12, 1327–1342.

[37] Strunin, M.A., Shmeter, S.M., 1996. Izvestia, Russian Academy of Sciences: Atmo- spheric Oceanic Physics. 32. American Geophysical Union, United States, pp. 29–35.

[38] Sunilkumar, S.V., Babu, A., Parameswaran, K., 2013. Mean structure of the tropical tropopause and its variability over Indian longitude sector. Clim. Dyn., 1125–1140. http://dx.doi.org/10.1007/s00382-012-1496-8.